Short Communication

Low Melting Point Glass Powder (glass) used as an Additive to $Zr_{0.88}Y_{0.08}Eu_{0.04}O_{2-\alpha}$ (ZYE) Electrolyte for Intermediate Temperature SOFCs

Ruijuan Shi[1], Wei Chen[2], Wenli Hu[2], Junlong Liu[1,*], Huiquan Li[1,*], Hongtao Wang[1,*], Liangquan Sheng[1]

[1] School of Chemical and Material Engineering, Fuyang Normal College, Fuyang 236037, China
[2] Fuyang Preschool Education College, Fuyang 236015, China
*E-mail: hongtaoking3@163.com, jlliu@fync.edu.cn, huiquanli0908@163.com

In this study, Eu^{3+} and Y^{3+} double doped ZrO_2, that is $Zr_{0.88}Y_{0.08}Eu_{0.04}O_{2-\alpha}$ (ZYE) electrolyte was synthesized by the chemical precipitation method. The low melting point glass powder (glass) was used as an additive to ZYE electrolyte for intermediate temperature SOFC after heated at 700 °C for 2 h. The phase composition and microstructure of the $Zr_{0.88}Y_{0.08}Eu_{0.04}O_{2-\alpha}$-low melting point glass powder (ZYE-glass) composite electrolyte were observed by XRD and SEM. The effects of gas atmosphere, operating temperature, time and the partial pressure of oxygen on the ionic conductivity of the ZYE-glass composite electrolyte were also studied at 400–800 °C.

1. INTRODUCTION

Hydrogen is widely recognized as the cleanest and most renewable energy source, and it can be used as a clean fuel in fuel cells, which are the most efficient tools for converting hydrogen energy into electrical energy. Solid oxide fuel cells (SOFCs) are proved to be one of the most important energy conversion devices because they exhibit high power-generation efficiency, multi-fuel capability and low emissions [1–6]. As an important component of SOFCs, solid electrolyte determines the efficiency of the SOFC and its operating conditions, such as working temperature. Yttria-stabilized zirconia (YSZ), which has good oxygen ionic conductivity, is the most extensively applied SOFC electrolyte material and is usually operated at high temperature (800–1000 °C) to minimize the ohmic and polarized losses. However, the conductivity of YSZ is significantly reduced when operating at lower temperatures (400–800 °C), which greatly limits its commercial application in SOFCs [7–12].

As has been found in many studies, double metal ion doped zirconia can effectively reduce the sintering temperature [13–15]. It has also been evidenced that double metal ion doped zirconia can significantly reduce the operating temperature and improve its conductivity. Gong et al. found that CaO/Y_2O_3-stabilized ZrO_2 exhibited higher ionic conductivity than ZrO_2-CaO and ZrO_2-Y_2O_3 at high temperature, which is mainly ascribed to the increase in the concentration of the oxygen vacancies [13]. It has been reported that doping Al_2O_3 to YSZ could enhance the mechanical properties, decrease the sintering temperature of YSZ, and the highest output value was achieved for a single cell based on 1 wt.% Al_2O_3-doped YSZ electrolyte [14]. YSZ-SDC (samarium doped ceria) composite was found to be responsible for the enhanced electrical conductivity in the temperature range 400-700 °C [15]. All this suggests that doping ZrO_2 with two different elements can improve conductivity. Metallic cation Eu^{3+} is similar to Y^{3+} in ionic radius and electronegativity. Therefore, we tried to fabricate a new dense composite electrolyte by using Eu^{3+} and Y^{3+} double doped ZrO_2 together with low melting point glass powder additive.

In this paper, a new ZYE-glass composite electrolyte was prepared. The structure, morphology, ionic conductivity and electrochemical properties at intermediate temperature (400–800 °C) of the composite electrolyte were examined by various methods. The effects of different gas atmospheres, operating temperature, time and the partial pressure of oxygen on the ionic conductivity were also studied.

2. EXPERIMENTAL

Eu^{3+} and Y^{3+} double doped ZrO_2, that is $Zr_{0.88}Y_{0.08}Eu_{0.04}O_{2-\alpha}$ (ZYE), electrolyte was prepared via the chemical precipitation method. To synthesize ZYE electrolyte, stoichiometric amounts of Y_2O_3 and Eu_2O_3 were dissolved in nitric acid and then added to the $Zr(NO_3)_4 \cdot 5H_2O$ solution under stirring. All the reagents used were of analytical-grade. The NH_4OH was added drop-wise to the mixed solution under continuous stirring until the *p*H reached 9. The precipitate was washed and dried. Subsequently, the resulting precursor was heated at 700 °C for 6 h to get the ZYE electrolyte. The ZYE electrolyte was mixed with low melting point glass powder (glass) at a weight ratio of ZYE electrolyte to glass of four to one. The composition of the low melting point glass powder is Na_2O-CaO-SiO_2-ZnO (Taizhou Xinhai Special Materials Factory, 300 mesh, m.p. is 550 °C). After heating at 700 °C for 2 h, the $Zr_{0.88}Y_{0.08}Eu_{0.04}O_{2-\alpha}$-low melting point glass powder (ZYE-glass) composite electrolyte was obtained.
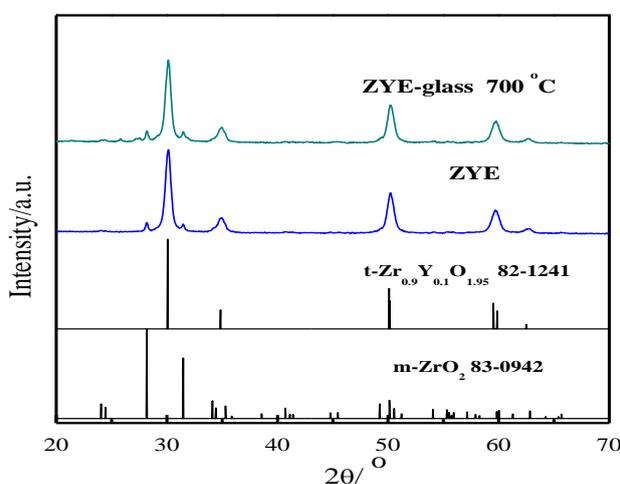
Thermogravimetry analysis and differential scanning calorimetry (TGA-DSC, Universal V 3.7A, TA Instruments, New Castle, USA) were analyzed to determine the suitable calcination temperature for the ZYE electrolyte. The precursor was heated in the temperature range of 25–1000 °C at the rate of 15 °C·min^{-1} with flowing N_2. The X–ray diffraction (XRD, X'pert Pro MPD, Amsterdam, Netherlands) patterns of the ZYE electrolyte and ZYE-glass composite electrolyte were obtained to determine the crystalline phase with a CuKα X-ray source (1.5418 Å). The morphology of the ZYE-glass composite electrolyte was investigated by a scanning electron microscope (SEM, S-4700, Hitachi, Tokyo, Japan).

　　　　The effect of different gas atmospheres, operating temperature, time and the partial pressure of oxygen on the electrical conductivities was investigated using an electrochemical analyzer (CHI660E, Shanghai, China) in a three-electrode system over the frequency range of 0.1 Hz to 1 MHz at 400–800 °C. And the ac amplitude was 20 mV. The sample powders were pressed into pellets and then ground into thin slices with a thickness of 1.0–1.2 mm. A 20% palladium-80% silver paste with silver wires were attached onto both sides of the pellets as electrodes, the areas of both electrodes were about 0.5 cm^2. A H_2/O_2 fuel cell using the ZYE-glass composite electrolyte as electrolyte was fabricated. The fuel cell was tested using the linear scanning of current and voltage method in the CHI660E electrochemical analyzer.

3. RESULTS AND DISCUSSION
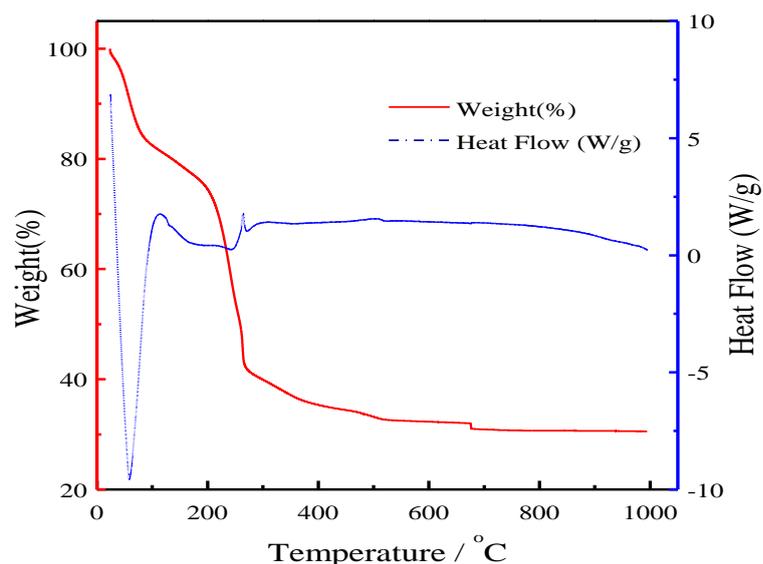
Figure 1. TGA-DSC curves of the precursor of ZYE electrolyte in nitrogen atmosphere up to 1000°C at 15 °C·min^{-1}.
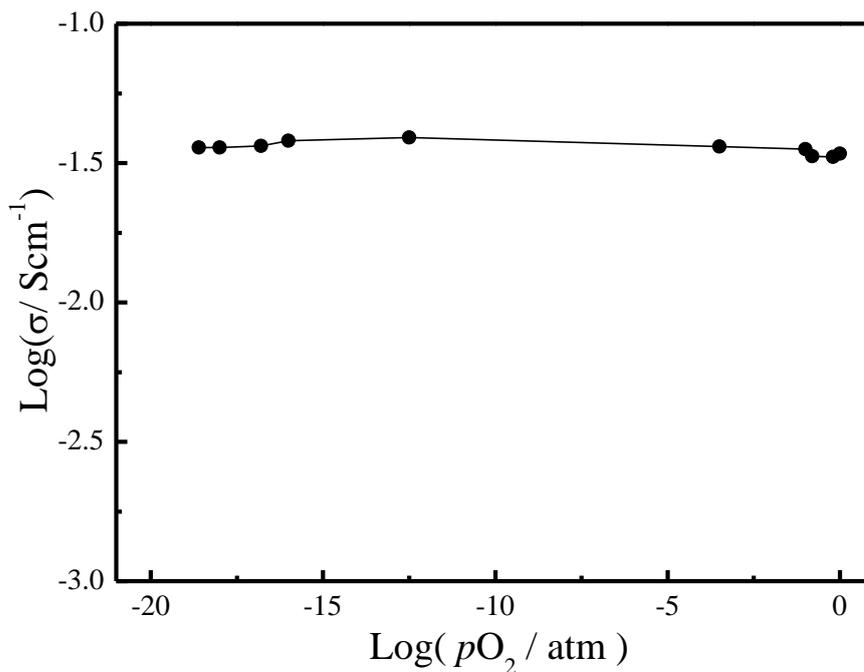

Figure 2. XRD patterns of the ZYE electrolyte and ZYE-glass composite electrolyte.

The thermogravimetry analysis and differential scanning calorimetry (TGA-DSC) were conducted to determine the suitable calcination temperature required for ZYE electrolyte. Fig. 1 shows the TGA-DSC curves of the precursor. As can be seen from Fig. 1, there was a weight loss of 15 % from room temperature up to 80 °C with a sharp endothermic peak which can be ascribed to the loss of the adsorbed water and ammonium salt in the precursor [16]. The DSC curve has two exothermic peaks between 100 °C and 300 °C accompanied by 40 % weight loss which can be assigned to the decomposition of the nitrate [17]. Almost no weight loss was observed when the temperature was above 680 °C, therefore, the optimal calcination temperature for ZYE electrolyte was chosen as 700 °C [18–19].
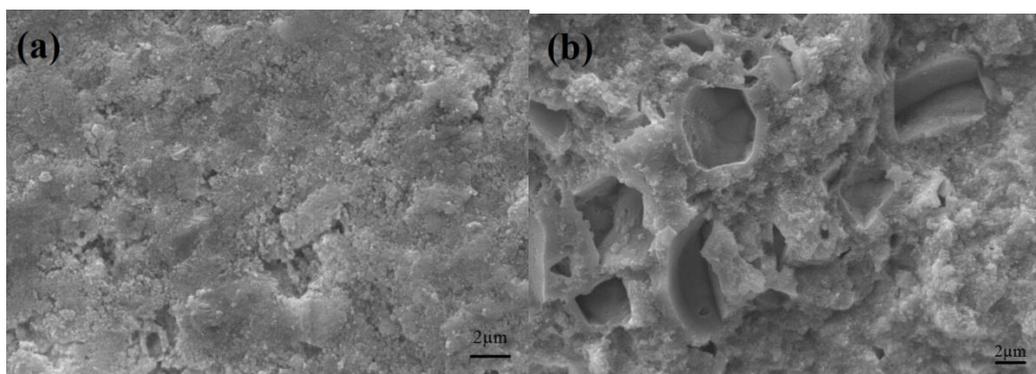
Figure 3. Surface (a) and cross-sectional (b) SEM images of the ZYE-glass composite electrolyte.
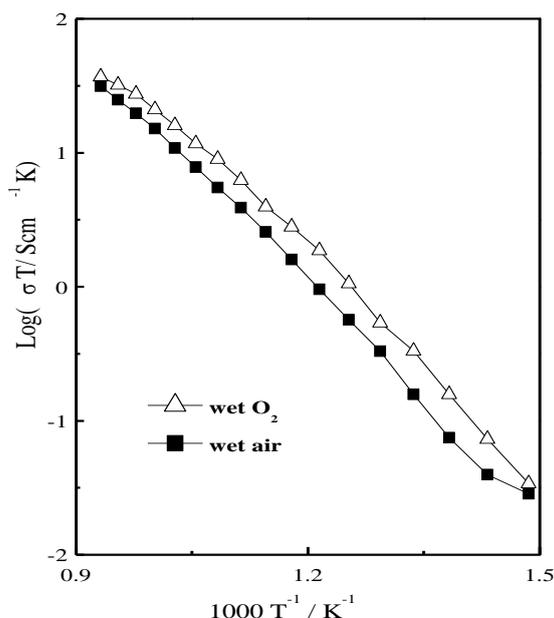

Figure 4. The conductivities of the ZYE-glass composite electrolyte as a function of the oxygen partial pressure (pO_2) range from 10^{-20} to 1 atm at 800 °C.

Fig. 2 shows the XRD diffraction patterns of the ZYE electrolyte and ZYE-glass composite electrolyte together with the standard data of t-$Zr_{0.9}Y_{0.1}O_{1.95}$ (JCPDS 82-1241) and m-ZrO_2 (JCPDS 83-0942). It is clear that both samples calcined at 700 °C possessed a mixture of t-$Zr_{0.9}Y_{0.1}O_{1.95}$ and m-ZrO_2 phases, where the tetragonal phase was the main constituent. And there were no characterized diffraction peaks relating to the low melting point glass powder phase, which means that the low melting point glass powder exists as an amorphous phase. All the results indicate that the low melting point glass powder which did not react with ZYE electrolyte mainly existed in the grain boundary in an amorphous form [20].

The microstructure of the ZYE-glass composite electrolyte was detected by SEM and the result is displayed in Fig. 3. Obviously, no visible pores or cracks were observed on the surface of the ZYE-glass composite electrolyte, which implies that the ZYE-glass composite electrolyte was fairly dense. However, it can be seen from Fig. 3(b) that some small scattered pores were found in the cross-sectional of the ZYE-glass composite electrolyte. It was also found that the pores were closed through the seal test and thus can not affect the electrochemical test.

Fig.4 shows the conductivities of the ZYE-glass composite electrolyte as a function of the partial pressure of oxygen. The conductivities of the ZYE-glass composite electrolyte were performed in the oxygen partial pressure (pO_2) range from 10^{-20} to 1 atm at 800 °C. It can be seen that the conductivities hardly changed with the partial pressure of oxygen in the whole pO_2 region, which demonstrates that the ZYE-glass composite electrolyte is a pure ionic conductor at 800 °C [21]. At 800°C, the molten low melting point glass powder may allow ionic charge carriers to move quickly and freely through it which is beneficial for the long-range transferability of ions.

Figure 5. The log (σT) $\sim$ 1000 T^{-1} plots of the ZYE-glass composite electrolyte in wet O_2 and wet air with a three-electrode system over the frequency range from 0.1 Hz to 1 MHz at 400–800 °C. And the ac amplitude was 20 mV.

The temperature dependence of the conductivities of the ZYE-glass composite electrolyte was measured in wet O_2 and wet air from 400 to 800 °C. As shown in Fig. 5, the log $(\sigma T) \sim 1000 \, T^{-1}$ plots of the ZYE-glass composite electrolyte exhibited a linear relationship and the conductivities were increased with increased temperature. The conductivities in a wet air atmosphere were slightly lower than that in wet O_2. The maximum conductivities of 3.4×10^{-2} S·cm^{-1} and 2.9×10^{-2} S·cm^{-1} were achieved in wet O_2 and wet air at 800 °C, respectively.
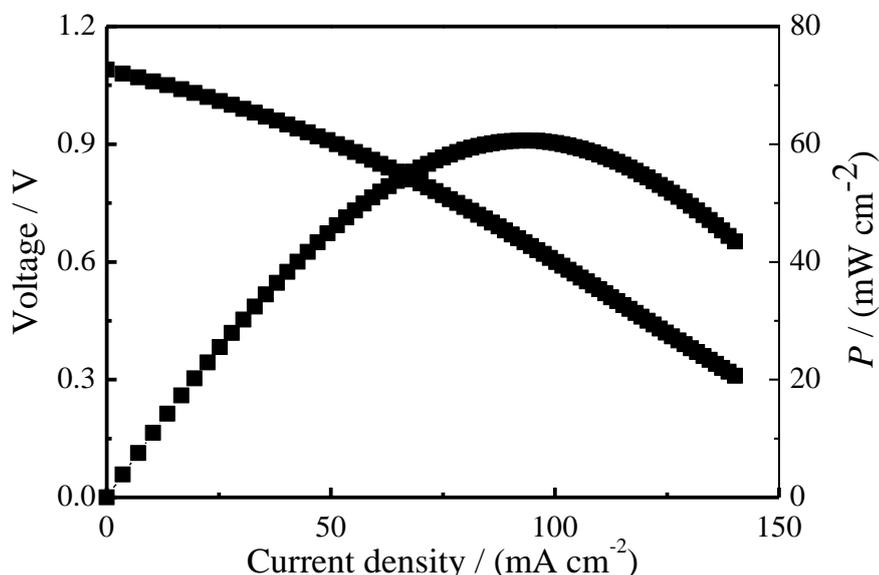
The stability of the ZYE-glass composite electrolyte was investigated by measuring the conductivities after a 17h run in a dry N_2 atmosphere. As shown in Fig. 6, the ZYE-glass composite electrolyte exhibited high and stable conductivity during the long run in a higher temperature range which was above the melting point of the low melting point glass powder (550 °C). This may be due to the ionic charge carriers being able to move quickly in the molten low melting point glass powder. However, the conductivity decreased slightly in the low temperature range. The glass is solid at 400–550 °C which hinders the mobility of ionic charge carriers, resulting in the decrease of electrical conductivity. It is suggested that the ZYE-glass composite electrolyte is stable enough for practical use in the high temperature range of 600-800 °C.
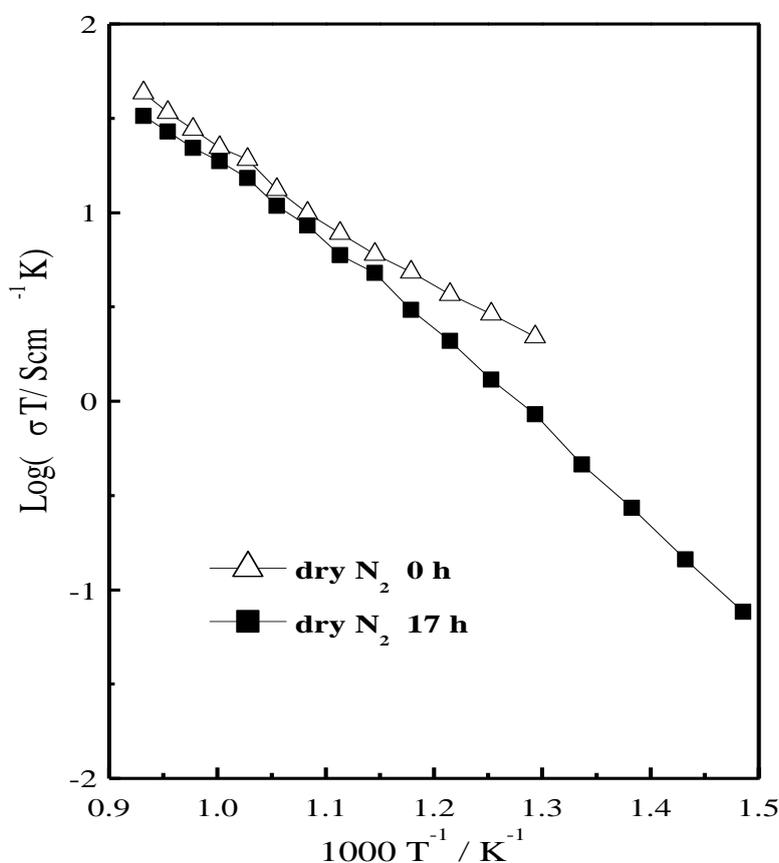
Figure 6. The log $(\sigma T) \sim 1000 \, T^{-1}$ plots of the ZYE-glass composite electrolyte in dry N_2 at the beginning of the experiment and after 17 h.

The fuel cell performance of the ZYE-glass composite electrolyte using H_2 as fuel and O_2 as oxidant was evaluated at 800°C and the result is shown in Fig. 7. As can be seen, the open circuit

voltage was 1.09 V which indicates that the ZYE-glass composite electrolyte is tight, and the maximum power output density is 60.6 mW·cm^{-2} at 800°C. Moon et al. found that a fuel cell with a YSZ thin film as the electrolyte showed a maximum power output density of 230 mW·cm^{-2} at 750 °C [22]. Lee et al. discovered that a YSZ membrane fuel cell using microemulsion-mediated and a conventionally ball-milled NiO-YSZ anode exhibited a maximum power output density of 362 mW·cm^{-2} and 160 mW·cm^{-2} at 850 °C, respectively [23]. The result is not so high as those reported on thin film fuel cells, which may be mainly ascribed to the electrolyte layer thickness (1.1 mm).

Figure 7. *I-V* and *I-P* curves of the H$_2$/O$_2$ fuel cell of the ZYE-glass composite electrolyte using the linear scanning of current and voltage method within the CHI660E electrochemical analyzer at 800 °C.

4. CONCLUSIONS

In this study, a new ZYE-glass composite electrolyte was prepared. The result of XRD indicates that the tetragonal is the main phase and low melting point glass mainly exists in the grain boundary in an amorphous form. The logσ ~ log (pO$_2$) plot illustrates that the ZYE-glass composite electrolyte is a pure ionic conductor at 800 °C. The highest conductivities are observed to be 3.4×10^{-2} S·cm^{-1} and 2.9×10^{-2} S·cm^{-1} in wet O$_2$ and wet air at 800 °C, respectively. The maximum power density of the ZYE-glass composite electrolyte (thickness = 1.1 mm) is 60.6 mW·cm^{-2} at 800 °C.

References

1. G. L. Liu, W. Liu Q. Kou and S. J. Xiao, *Int. J. Electrochem. Sci*., 13 (2018) 2641.
2. R. Shi, J. Liu, H. Wang, F. Wu, and H. Miao, *Ceram. Int.*, 43 (2017) 16931.
3. T. Hibino, K. Kobayashi, P. Lv, M. Nagao, S. Teranishi, and T. Mori, *J. Electrochem. Soc.*, 164 (2017) F557.
4. Y. N. Chen, T. Tian, Z. H. Wan, F. Wu, J. T. Tan and M. Pan, *Int. J. Electrochem. Sci.*, 13 (2018) 3827.
5. S. Lee, and X. Guan, *MRS Communications*, 7 (2017) 199.
6. J. Luo, A.H. Jensen, N.R. Brooks, J. Sniekers, M. Knipper, D. Aili, Q. Li, B. Vanroy, M. Wübbenhorst, F. Yan, L.V. Meervelt, Z. Shao, J. Fang, Z.-H. Luo, D.E.D. Vos, K. Binnemans, and J. Fransaer, *Energy Environ. Sci.*, 8 (2015) 1276.
7. A. Dankeaw, G. Poungchan, M. Panapoy, and B. Ksapabutr, *Sensor. Actuat. B: Chem.*, 242 (2017) 202.
8. X.Y. Liu, Z.H. Xu, and G.Y. Liang, *Mater. Lett.*, 191 (2017) 108.
9. N. Mamana, A. Díaz-Parralejo, A.L. Ortiz, F. Sánchez-Bajo, and R. Caruso, *Ceram. Int.*, 40 (2014) 6421.
10. F.R. Bueta, J.F. Imperial, and R.B. Cervera, *Ceram. Int.*, 43 (2017) 16174.
11. A. Elmouwahidi, E. Bailón-García, A.F. Pérez-Cadenas, F.J. Maldonado-Hódar, J. Castelo-Quibén, and F. Carrasco-Marín, *Electrochim. Acta.*, 259 (2018) 803.
12. O. Bohnke, V. Gunes, K.V. Kravchyk, A.G. Belous, O.Z. Yanchevskii, and O.I. V'Yunov, *Solid State Ions.*, 262 (2014) 517.
13. J. Gong, Y. Li, Z. Tang, and Z. Zhang, *Mater. Lett.*, 46 (2000) 115.
14. L. Lei, Y. Bai, and J. Liu, *J. Power Sources*, 248 (2014) 1312.
15. Raghvendra, and P. Singh, *Ceram. Int.*, 43 (2017) 11692.
16. A. Matsuda, S. Oh, V.H. Nguyen, Y. Daiko, G. Kawamura, and H. Muto, *Electrochim. Acta*, 56 (2011) 9364.
17. M.T. Soo, N. Prastomo, A. Matsuda, G. Kawamura, H. Muto, A.F.M. Noor, Z. Lockman, and K.Y. Cheong, *Appl. Surf. Sci.*, 258 (2012) 5250.
18. M.I.G. Miranda, C.I.D. Bica, S.M.B. Nachtigall, N. Rehman, and S.M.L. Rosa, *Thermochim. Acta*, 565 (2013) 65.
19. S. Huang, and J.J. Sheng, *Fuel*, 210 (2017) 98.
20. M. Keane, and P. Singh, *Ceram. Int.*, 40 (2014) 7261.
21. J. Liu, R. Du, R. Shi, and H. Wang, *Ceram. Int.*, 44 (2018) 5179.
22. H. Moon, S.D. Kim S.D, S.H. Hyun, and H.S. Kim, *Int. J. Hydrogen Energ.*, 33 (2008) 2826.
23. M.K. Rath, Y.M. Jung, J.H. Park, D. W. Joh, and K.T. Lee, *J. Alloy Compd.*, 723 (2017) 681.